

Multi-terminal capacitor sensors†

W Chr Heerens

Delft University of Technology, Department of Applied Physics,
Lorentzweg 1, 2628 CJ Delft, The Netherlands

Received 12 March 1981, in final form 22 May 1981

Abstract. A survey is given of the theoretical background for designing multi-terminal capacitor sensors† of several types, suitable for control of every physical quantity that can be related with the change in position of two carriers, covered with electrodes. Previously published investigations of capacitor sensors, are briefly mentioned, and a description of the capacitance bridge used and the results of investigations of a multi-terminal capacitor test model are given. The main conclusion is that the capacitor sensors described can be used in cases where reliability and sensitivity of laser interferometry and strain gauge measurements fail.

1. Introduction

Theoretical expressions for the description of the capacitance of a homogeneously filled capacitor can be collected in one basic expression:

$$C = \epsilon f(G) \quad (1)$$

where

C is the capacitance in farads

ϵ is the permittivity of the material, filling the space of the capacitor, in farads per metre

$f(G)$ is a geometry-depending factor with the dimension of length in metres.

The permittivity of the material is divided into two main factors:

ϵ_0 the permittivity of vacuum, being a physical constant $8.854 \dots 10^{-12} \text{ Fm}^{-1}$

ϵ_r the relative permittivity of the material, filling the capacitor and being dimensionless ($\epsilon_{r,\text{vacuum}} = 1$).

In principle the most simple geometry depending factor $f(G)$ is given by only one length, multiplied by a constant factor. However, a closer look into electricity shows that the presence of all conductors in the environment influences the capacitance between the two conductors, forming the capacitor. One of the first capacitors, to be constructed and investigated in the 19th century, was the parallel plate capacitor (figure 1), consisting of two parallel plates with equal surfaces O and a separation distance d .

In this case the geometry-depending factor $f(G)$ is approximately given by

$$f(G) = O/d. \quad (2)$$

This is only an approximation because fringes, surfaces of the back of the plates and connecting wires do contribute to the total capacitance between the two conductors.

For the parallel plates capacitor Kelvin (Maxwell 1873) has given in principle the solution of this problem by introducing a third electrode, the guard-ring. This guard-ring encloses, in a coplanar way, one of the plate electrodes (the island electrode),

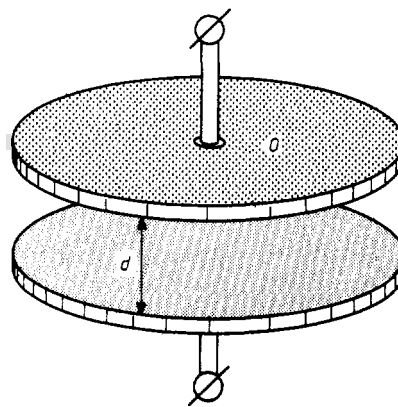


Figure 1. The simple parallel plate capacitor.

while the other electrode is enlarged in its sideways dimensions (figure 2). If the width of the gap between the island electrode and the guard-ring is extremely small, compared with the electrode distance d , the capacitance C between the island and the opposite electrode can be calculated with high accuracy, using the ideal parallel plate capacitor formula:

$$C = \epsilon_0 \epsilon_r O/d. \quad (3)$$

Experiments by Moon and Sparks (1948), Brown and Bulleid (1978) and theoretical and experimental investigations of the author (Heerens and Vermeulen 1975) give more details about the original Kelvin guard-ring capacitor.

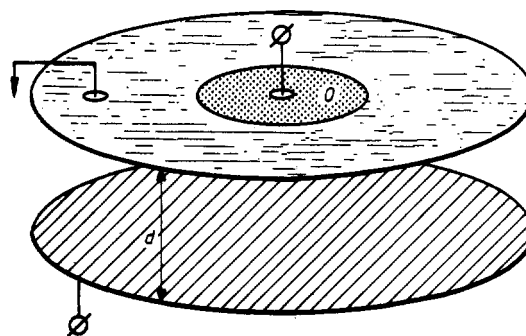


Figure 2. The Kelvin guard-ring capacitor.

2. Theoretical background

In order to achieve the rules for designing multi-terminal capacitors, one has to solve Laplace's equation in the concerned geometry. In geometries, where one of the three dimensions can be called infinite, compared with the other two, the Laplace equation has become a two dimensional and linear one. This equation can be solved in several electrode geometries by using complex function theory and conformal transformations. These calculations, followed by surface charge density calculations, finally result in capacitance calculations. Figure 3 shows the cross section of the capacitor geometry, where, according to principles formulated by Thompson and Lampard (1956), present primary standards of capacitance are based on standardisation offices like NBS and the Canadian NRC.

If the two possible cross capacitances per length l are equal,

† Patent pending in Europe (10 countries), USA, Canada and Japan.

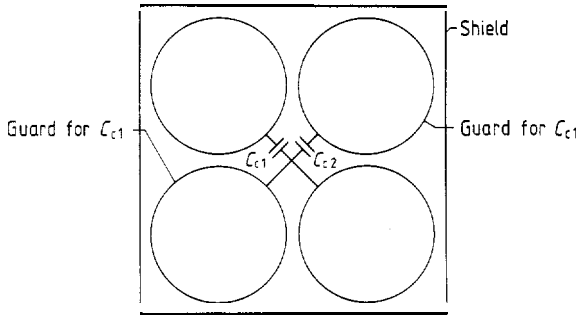


Figure 3. Cross section of the Thompson-Lampard standard capacitor.

then this capacitance is given by:

$$C_c = \epsilon_0 \epsilon_r (\ln 2/\pi) l. \quad (4)$$

The geometry factor in this equation corresponds to the most simple one mentioned before. However in practice, due to finite length of the capacitor devices, fringe effects do exist.

Cylindrical and toroidal configurations with rectangular sectional shapes are geometries, where Laplace's equation is not linear and yet the solution in analytical form is of great importance. In the cases where the potential distribution on the boundaries is rotationally symmetrical, complete analytical solutions have been found by the author (Heerens 1976).

Using analytical surface charge density calculations and capacitance calculations in a more universal form, calculations of several special capacitor geometries, including gap effects, are published by the author (Heerens 1979, Heerens *et al* 1979).

For practical capacitor sensor designs the following survey of special geometries is of importance (figures 4 and 5). The smallest circular cross capacitance in figure 4 is:

$$C_{c1} = \epsilon_0 \epsilon_r \frac{4\pi R_1 R_2}{d} \sum_{n=1}^{\infty} (-1)^{n+1} I_1(n\rho_1) K_1(n\rho_2) \quad (5)$$

where I_1 and K_1 are first order modified Bessel functions and where for ρ_1 and ρ_2 they can be written as $\pi R_1/d$ and $\pi R_2/d$ respectively. The largest cross capacitance is:

$$C_{c2} = C_{c1} + \epsilon_0 \epsilon_r \pi (R_2^2 - R_1^2)/d. \quad (6)$$

If $R_1 = R_2 = R$, after finite series expansions and the use of Euler-series, equations (5) and (6) result in:

$$C_c = \epsilon_0 \epsilon_r (\ln 2/\pi) 2\pi R [1 + 0.000\ 043\ 507(d/R) - 0.050\ 631\ 437(d/R)^2 + \dots], \quad (7)$$

which is in fact the circular analogon of the linear

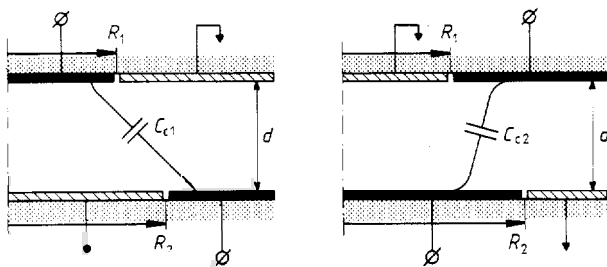


Figure 4. Radial cross sections of circular cross capacitors.

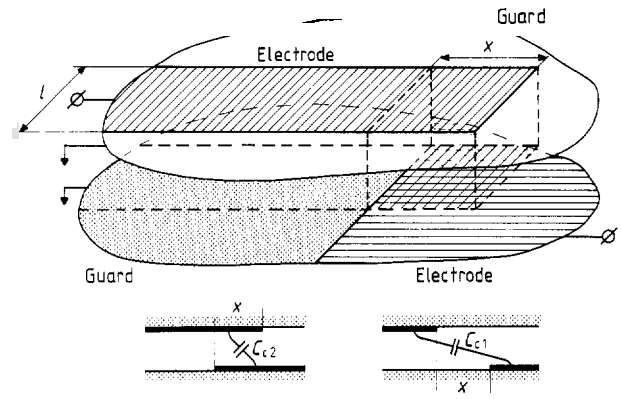


Figure 5. Schematical view of practical cross capacitors.

Thompson-Lampard capacitor, but now without fringe effects. The contribution of the (d/R) term is caused by the used finite series expansions, while in infinite series expansions the (d/R) term does not exist.

The asymptotic expansions for extremely large value of R , compared with d , of the capacitance per length of arc l (as a part of the circle surrounding $2\pi R$) results in an equation similar to that of Lampard (equation (4)).

The configuration, according to figure 5 is another interesting asymptotic expansion, derived from equations (5) and (6) for large values of R_1 and R_2 .

Both capacitance equations are:

$$C_{c2} = (\epsilon_0 \epsilon_r l/\pi) \{ \ln [2 \cosh(\pi x/2d)] + \pi x/2d \} \quad (8)$$

$$C_{c1} = (\epsilon_0 \epsilon_r l/\pi) \{ \ln [2 \cosh(\pi x/2d)] - \pi x/2d \} \quad (9)$$

where

$$x = R_2 - R_1,$$

with resulting special situation for $x = 0$:

$$C_{c1} = C_{c2} = C_c = \epsilon_0 \epsilon_r l (\ln 2/\pi). \quad (10)$$

Rules for the dimensions of gaps and the limitation of the dimensions of parts of the electrodes can also be achieved in a fundamental analytical way. In practice this results in ratios like gapwidth/electrode-distance equal $\frac{1}{2}$ and electrode-distance/side-way-limitations equal $\frac{1}{2}$ for 1 PPM accuracies. Finally the places can be indicated where wires must be connected, without having influences on accuracy.

All these rules result in calculation accuracies for capacitor sensors within the tolerances with which the sensors will be manufactured.

3. Basic types of capacitor sensors and practical values of capacitances

If the earlier mentioned rules for designing capacitor sensors are obeyed, the following basic types can be obtained:

Parallel plate capacitor (figure 6(a))

$$C_{pl} = \epsilon_0 \epsilon_r b l/d. \quad (11)$$

The capacitance C_{pl} is reciprocal to the electrode distance d .

Single cross capacitor (figure 6(b))

$$C_{sc} = \epsilon_0 \epsilon_r (\ln 2/\pi) l. \quad (12)$$

The capacitance C_{sc} is proportional to common length l .

Differential plate capacitor combination (figure 6(c))

$$C_1/C_2 = d_2/d_1. \quad (13)$$

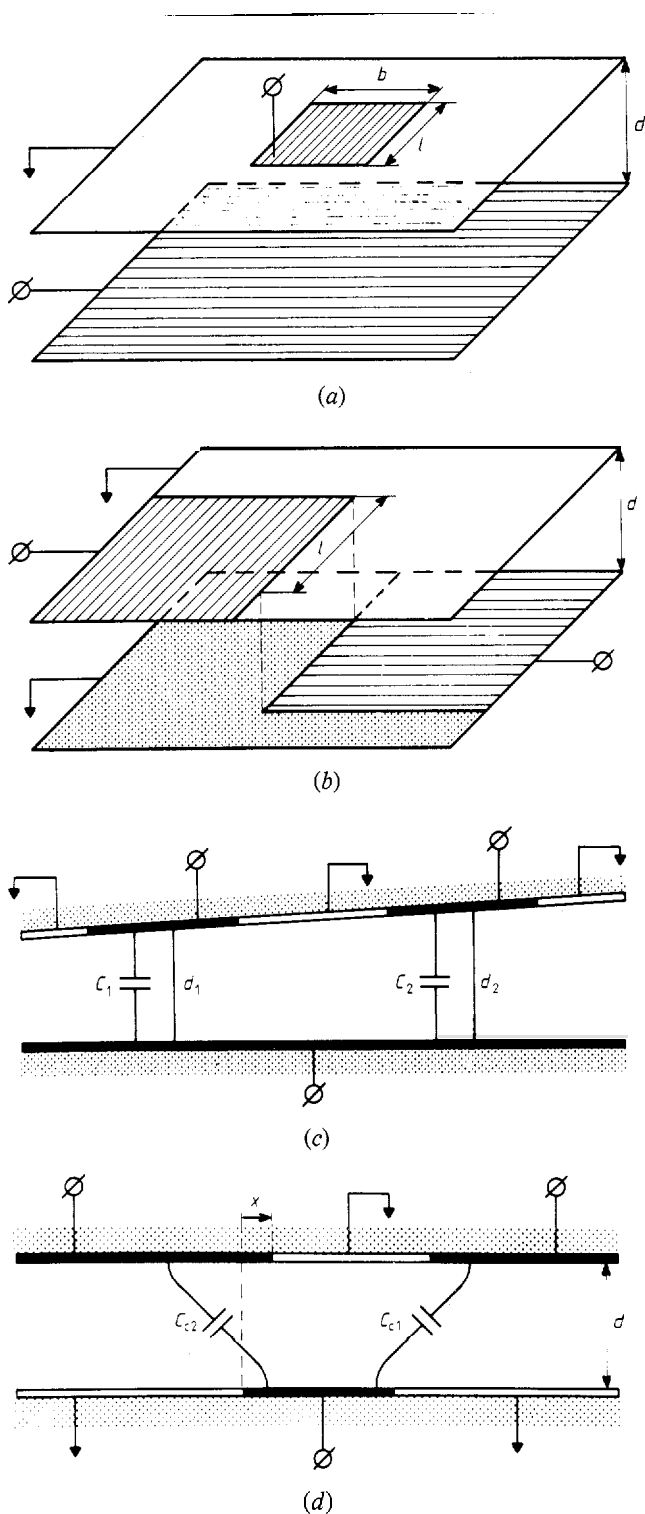


Figure 6. Basic types of multi-terminal capacitors. (a), Parallel plate capacitor; (b), single cross capacitor; (c), differential plate capacitor combination; (d), differential cross capacitor combination.

The capacitance ratio C_1/C_2 is reciprocal to the ratio of local distances d_1 and d_2 , if d_1 is approximately equal d_2 .

Differential cross capacitor combination (figure 6(d))

$$C_{c2} - C_{c1} = \epsilon_0 \epsilon_r (l/d)x. \quad (14)$$

The difference in capacitance $C_{c2} - C_{c1}$ is proportional to a sideways displacement x .

Practical values of capacitance are 1–100 pF for parallel plate capacitors and 2 pF m^{-1} for cross capacitances.

With modern capacitance bridge circuits, based on the use of ratiotransformers, capacitances of 10^{-7} to 10^{-8} pF can be measured.

4. A survey of the capacitance bridge principle

Basically the capacitor sensors are of the three terminal type, so a capacitance bridge circuit equipped for these kind of capacitors must be used. Either a single capacitor will be compared with an external standard capacitor or a two element differential capacitor will be connected with bridge terminals.

Figure 7 shows the principles of a well dimensioned capacitance bridge. A low impedant AC-generator G drives the primary winding of a 1:1 shielded bridge transformer T . The central tap CT of the secondary winding is used as central ground. A decade transformer is connected between CT and one of the ends I of the secondary winding of the bridge transformer. The capacitor to be measured, C_x , has one terminal connected with the other end C . One of the connectors of the reference capacitor C_r is connected with the variable tap DT , positioned at place x of the decade transformer. The other connectors of both capacitors are together connected with the lock-in amplifier D , while all guard electrodes and shields are connected with CT .

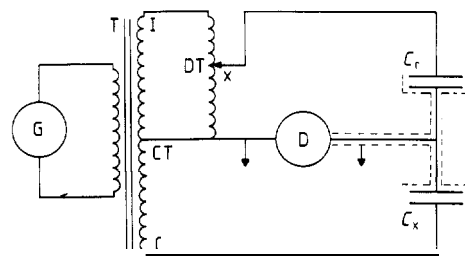


Figure 7. Principle of three-terminal bridge circuit.

Figure 7 can be substituted by the scheme of figure 8, where the parasitic capacitances are marked in dashed lines. Due to the low impedant voltage sources xV and V , compared with all other impedances in the circuit, there is no influence of the parasitic capacitances C_{p1} and C_{p2} , acting as loads for the voltage sources.

If the bridge is used as zero-indicating instrument, by

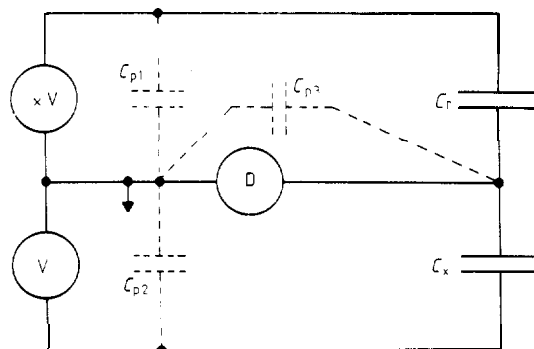


Figure 8. Basic bridge principle for elimination of parasitic capacitances.

Table 1. Summary of bridge/electrode connections for all six degrees-of-freedom operation modes.

Operation mode	Bridge terminals (figure 7) connected with electrode terminals (figure 9)				DT	Detector	According type of capacitor (figure 6)	See also part of (figure 10)
	I	C	CT	DT				
translation x-direction	—	B	D, E, F, G, K	A, C	H, J	6(b) 4x	10(a)	
translation y-direction	D	E	A, B, C, F, G, H, J	†	K	6(d)	10(e)	
translation z-direction	—	D, E, F, G	A, B, C, K	†	H, J	6(a) 4x	10(d)	
rotation around x-axis	D	E	A, B, C, F, G, K	†	H, J	6(c)	10(b)	
rotation around y-axis	D, E	F, G	A, B, C, K	†	H, J	6(c) 2x	10(c)	
rotation around z-axis	D, F	E, G	A, B, C, H, J	†	K	6(d) 2x	10(f)	

† External standard capacitor connected with DT for reference measurements.

making the detector current zero, the parasitic capacitance C_{p3} , acting as a shunt of the detector, only has an influence on bridge sensitivity but not on the accuracy.

5. Design and investigations of a six-degrees-of-freedom test model, as an example

Apart from the investigations of the use of this type of capacitor sensors in an absolute membrane differential pressure gauge by the author Heerens (1979), van Kessel and van der Straaten (1980) and in an absolute thickness monitor by Keizer (1980), a multi degrees-of-freedom capacitor sensor has been designed and investigated.

Figure 9 shows the design of that test model, where figure 9(a) shows the geometry of the voltage driven electrodes, while figure 9(b) shows the geometry of the detector electrodes on the opposite electrode carrier. The electrodes are formed by vapour deposition on polished glass, followed by photolithography of the patterns and etching of gaps. Both electrode carriers are mounted in shielding boxes and, with optical positioning devices, supported by an optical rail system, suitable for laser interferometry.

If electrodes D, E, F and G are connected with bridge transformer terminal C (see figure 7) and electrodes H and J are connected with the detector, while all other electrodes are connected with CT, a comparison with a standard capacitor in the other bridge arm as reference capacitor gives the measurement of the mean distance between the two electrode carriers.

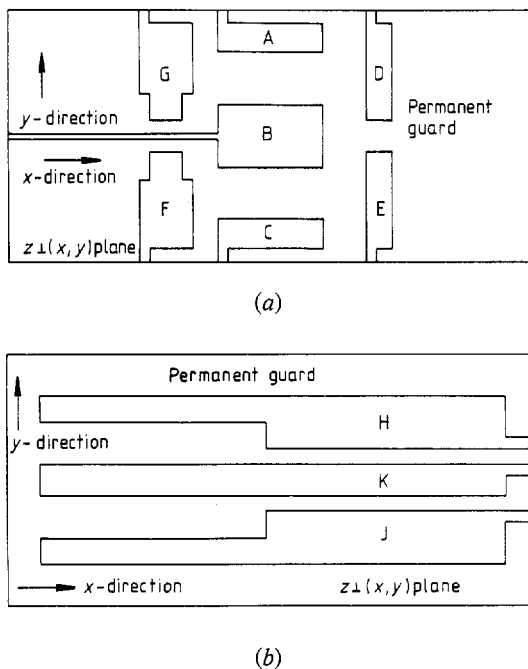


Figure 9. Six-degrees-of-freedom capacitor design: (a), design of voltage driven electrodes surrounded by a guard; (b), design of detector electrodes surrounded by a guard.

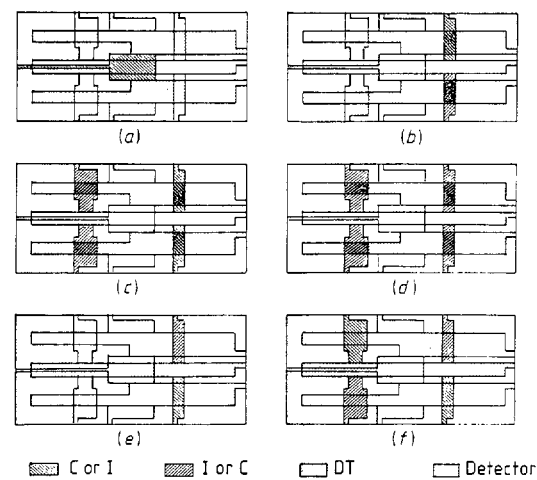


Figure 10. Schematic transparent top view of electrode connections for the six-degrees-of-freedom test model. (a), translation in x-direction (compared with internal reference); (b), rotation around x-axis; (c), rotation around y-axis; (d), translation in z-direction; (e), translation in y-direction; (f), rotation around z-axis.

Also other connections of electrodes can be chosen and in fact all six degrees-of-freedom between the two electrode carriers can be measured.

In table 1 a summary is given of bridge/electrode connections for all six degrees-of-freedom. Figure 10 gives a transparent top view of the formed capacitors per degree-of-freedom mode.

In table 2 the performances of the test model are given.

Table 2. Performance characteristics of the six-degrees-of-freedom test model capacitor sensor.

Translation direction	Resolution (nm)	Range (mm)
<i>x</i>	40	20
<i>y</i>	11	6
<i>z</i>	0.12	2.5
Axis of rotation	Resolution in angle (rad)	Resolution in angle (deg)
<i>x</i>	5×10^{-8}	2×10^{-6}
<i>y</i>	3×10^{-8}	10^{-6}
<i>z</i>	5×10^{-7}	2×10^{-5}

The resolution in all modes is so good that small bending and torsion of the heavy and stable optical rail system, due to the temperature gradients and external momenta created, could be measured even in the situations where laser interferometry and strain gauge measurements do not give results anymore.

6. Conclusions

Basically the use of these capacitor sensors concern all physical quantities which, in some way, can be related with the change in position of two carriers, covered with electrodes, or with the change in dielectric properties of materials in the space between the electrodes.

Several capacitor sensors for various applications have been designed and tested in the laboratory in the last few years. For these sensors there was full agreement between theory and practice within the manufacturing tolerances, even if relative tolerances of approximately 10 parts per million were used. The main conclusions are:

- (i) In most of the sensor designs there is a linear relation over the entire range between the quantity to be controlled and the output of the sensor.
- (ii) The input/output relation can be precalculated.
- (iii) Reference gauges can be built in the sensor itself, which increases stability, while the output signal becomes a dimensionless fractional number.
- (iv) Mixing of bridge systems with different bridge frequencies for simultaneous detection up to six-degrees-of-freedom with one modified sensor system is possible.
- (v) In comparison with laser interferometrical systems much smaller details can be measured (sometimes less than a nanometer) and the system is, due to linear input/output relations, easier to handle.
- (vi) In comparison with strain gauges the capacitor sensor system is much more sensitive and less temperature dependent.

Acknowledgments

The author thanks his assistant and partner in patent pending activities G H Peerbolte for his impressive technical contribution to the achieved know-how in multi-technical capacitor sensor

designs and his esteemed colleague and teacher O F Z Schannen for his constructive comments in the instrumentation of the capacitance bridges.

The author also thanks his students B Cuperus, R Hommes, G Keizer, J C M van Kessel, J H W van der Straaten and F C Vermeulen for their enthusiastic and helpful cooperation in investigations during the last years.

References

- Abramowitz M and Stegun I A 1965 *Handbook of Mathematical Functions* (New York: Dover)
- Brown M A and Bulleid C E 1978 The effect of tilt and surface damage on practical capacitance displacement transducers *J. Phys. E: Sci. Instrum.* **11** 429–32
- Heerens W Chr 1976 The solution of Laplace's equation in cylindrical and toroidal configurations with rectangular sectional shapes and rotation-sy *J. Appl. Phys.* **47** 3740–4
- Heerens W Chr 1979 *Theory and practice of the absolute membrane differential pressure gauge, Dissertation Delft* (in Dutch)
- Heerens W Chr, Cuperus B and Hommes R 1979 Capacitance of Kelvin guard-ring capacitors with modified edge geometry *Delft Progr. Rep.* **4** 67–81
- Heerens W Chr and Vermeulen F C 1975 A new theorem in electrostatics and its application to calculable standards of capacitance *J. Appl. Phys.* **46** 2486–90
- Keizer G 1980 *An absolute capacitor thickness monitor, Master Thesis Delft* (in Dutch)
- Kessel J C M van and Straaten J H W van der 1980 *A bakeable absolute membrane differential pressure sensor with electronic control and signal processing, Master Thesis Delft* (in Dutch)
- Maxwell J C 1873 *A Treatise on Electricity and Magnetism* vol 1 (Oxford: Clarendon)
- Moon C and Sparks C M 1948 Analytical formulas for toroidal cross capacitances with rectangular sectional shapes including gap correction formulas *J. Res. Nat. Bur. Stand.* **41 RP 1935** pp 497–507
- Thompson A M and Lampard D G 1956 Standards for low values of direct capacitance *Nature* **177** 888